

Seismic Detection of Cold Production Footprints of Heavy oil in Lloydminster Field

Sandy Chen*, Larry Lines, Joan Embleton, P.F. Daley
Department of Geology and Geophysics, University of Calgary,
2500 University Dr. NW, Calgary, AB, T2N 1N4
qschen@ucalgary.ca

and

Larry Mayo
EnCana Corporation, Calgary, Alberta

ABSTRACT

The simultaneous extraction of oil and sand during the cold production of heavy oil generates high permeability channels termed “wormholes”. The development of wormholes causes reservoir pressure decrease to the bubble point, resulting in dissolved-gas within live heavy oil out of solution to form foamy oil. The foamy oil could fill depressurized drainage regions (production footprints) around the borehole, leading to fluid phase changes with gas bubbles in these regions. The Gassmann equation has been employed to calculate the bulk modulus variations of the drainage rocks, where the velocity and density decrease dramatically due to some exolved gas. In this paper, a 2D cold production model has been built to examine the seismic responses of drainage regions based on well logs in Lloydminster cold production pool. The seismic modeling responses indicate the amplitude anomalies and traveltimes delays in these regions upon comparison of pre and post production results. However, because most heavy oil cold production reservoirs are very thin, with less than 10m of net pays, seismic resolution is a challenge. Different seismic frequency bandwidths have also been tested to look at how vertical seismic resolution determines the detections of the drainage regions.

1. Introduction

The extracted cold production of heavy oil is a non-thermal process, in which sand and oil are produced simultaneously to enhance the oil recovery. This process has been economically successful in several unconsolidated heavy oil fields in Alberta and Saskatchewan. Compared with that from the non-sand production process, the oil recovery with sand production has been dramatically improved. The reason for this is that producing sand creates a foamy oil drive and a wormhole network. And these two effects are keys to boost the oil recovery.

1.1 Wormhole Network Growth

During the cold production process, heavy oil and sand are dragged to the surface together using progressive cavity pump, generating sharp pressure

gradients in the reservoir. This results in a failure of the unconsolidated sand matrix. The failed sand flows to the well, triggering the development of wormholes. Sawatzky and Lillico (2002) believe that wormholes grow in unconsolidated, clean sand layers within the net pay zone, along the highest pressure gradient between the borehole and the tip of the wormhole. They usually can grow to a distance of 150 m or more from the original wells, and form approximately horizontal high permeability channels connecting wells in the reservoirs.

Based on the laboratory experiments conducted by Alberta Research Council (ARC), Tremblay, et al (1999) observed that the porosity of the mature wormholes could reach 50% or more. He also determined wormhole diameters could range from the order of 10cm to one meter as the maximum size. Wormholes play an important role to improve the permeability of the reservoir, but Sawatzky believes that the wormhole density cannot exceed 5% of total net pay. In this case, the wormhole contribution to the average porosity of the net pay is relatively small.

1.2 Foamy Oil Drive

The cold production process involves the depressurization of the live heavy oil in the reservoir. When sands and heavy oil are produced simultaneously and wormholes grow, the pressure declines to below the bubble point, resulting in the exsolution of dissolved gases as bubbles within the oil. The viscosity and gravity of heavy oil restrict the gas bubbles from coalescing into a separate phase. Thus, the trapped gas bubbles within the heavy oil form the foamy oil. The formation of foamy oil increases the fluid volume within the reservoir, forcing grains apart (Figure 1a), and driving both oil and gas to the wells through wormholes (Figure 1b). Therefore, foamy oil within the reservoir reduces the viscosity of heavy oil and improves oil recovery.

1.3 Drainage Footprints

The drainage region could be considered as the region that is depressurized or from which the oil is produced. In cold production, when wormholes are generated, the pressure around the wormholes decreases dramatically, leading to the drainage region expanding at least as far as the extent of wormholes through the entire net pay. Most net pay zones in cold production are on average less than 7m thick (Sawatzky and Lillico, 2002). The drainage region can be simplified as a cylinder around the borehole. Figure 2 shows a 3D plane view and a 2D cross section of the drainage region. The drainage region with a lower pressure has been filled with foamy oil. The average change of porosity in the drainage region is very small compared with the ambient rocks due to the small density of wormholes. However, the drainage region has still been highly disturbed from the initial state of the reservoir because of the presence of foamy oil. Sawatzky and Lillico (2002) showed a most likely drainage footprint scenario for the cold production wells in the small southwest Saskatchewan heavy oil pool

(Figure 3), where drainage regions are approximately elongated around the borehole.

Engineers believe that 3D time-lapse seismology could be a tool implemented in the imaging of the drainage region, caused by foamy oil and the presence of wormholes. Based on the laboratory experiments, Domenico et al. (1976) demonstrated that the compressional velocity (V_p) drops significantly with the presence of a small amount of gas in the pore fluid, which commonly caused “bright spots” on seismic responses. Mayo (1999) also showed some amplitude anomalies caused by foamy oil around the boreholes in a 3D time-lapse seismic survey from cold production in the Lloydminster area, which could represent the drainage regions (Figure 4).

2. Numerical Models Of Cold Production Reservoirs

2.1 Geological Model

Before production, the geological model was built based on the logs from one well drilled by EnCana Corporation in the Lloydminster heavy oil cold production pool. The production zone is the McLaren Formation consisting of unconsolidated sandstones in the Upper Mannville BB Pool. According to the density, gamma ray and P-wave velocity (converted from sonic) logs, a geological model of the initial reservoir has been built and is shown in Figure 5. This model is 1000m by 1000m in the horizontal and vertical directions, consisting of four layers matched the variations of well logs. From top to bottom, layer 1 is defined from the surface to the top of Mannville Formation at 726 m with a velocity of 2496m/s and a density of 2.26g/cm³; layer 2 is from the top of Mannville Formation to the top of the McLaren Formation at 742 m with a velocity of 3227m/s and a density of 2.37g/cm³; layer 3, the production formation, with a velocity of 2795m/s and a density of 2.16g/cm³, is from the top of McLaren Formation to 760 m, instead of the bottom of the McLaren Formation. The reason for this is because there are sharp variations in both density and velocity logs at the bottom of McLaren Formation, which are probably due to the highly cemented sand. Layer 4 starts from 760 m to the bottom of the model at 1000 m with a velocity of 3261m/s and a density of 2.4g/cm³. The interval velocities and densities of each layer except layer 4 are calculated from logs corresponding to their depths. The interval velocity and density of layer 4 are the averages from 760 m to 800 m on the logs.

From the porosity, gamma ray and resistivity logs, we can see that there are two main preferred net pay zones in the McLaren Formation. One is from 745m to 750m and the other from 755m to 758m. During production, wormholes would likely grow within the two pay layers, where the drainage regions can be expanded and filled with foamy oil. Assuming that the wormholes can extend 100m and 150m from the well in each pay zone respectively, the diameters of the drainage region will be 200 m and 300 m through the entire pays. We have

considered a drainage region as a cylinder in 3D domain, and a 2D model is illustrated in Figure 6.

2.2 Physical Properties Of Drainage Regions

Before production, the drainage regions have no difference in velocity and density with the ambient reservoir rocks. However, during or after the start of production, the reservoir fluids in the drainage regions have changed to three phases of oil, gas (in foamy oil), and water from the two phases of oil and water which were before production. With fluid phase changes, the Gassmann equation (1951) is employed to calculate the saturated rock bulk modulus (K_u),

$$K_u = K_d + \frac{(1 - K_d/K_s)^2}{\frac{\phi}{K_f} + \frac{1 - \phi}{K_s} - \frac{K_d}{K_s^2}} \quad (1)$$

where, K_d , K_s , K_f , and ϕ are the dry rock bulk modulus, the solid grain modulus, the fluid bulk modulus and the porosity. The shear bulk modulus of saturated rock is derived from the method provided by Bentley and Zhang (1999). And the saturated rock bulk density can be calculated as:

$$\rho_u = \rho_s(1 - \phi) + \rho_f\phi \quad (2)$$

where ρ_s , ρ_u and ρ_f are the densities of solid grains, saturated reservoir rock and fluid mixture at reservoir conditions.

To approximate the bulk modulus K_f of the fluid mixture, an assumption has to be made that the fluids are mixed uniformly at a very fine scale with gas bubbles trapped within the heavy oil. In this situation, any small amount of gas will cause the estimate of the fluid mixture bulk modulus to be very low. Then the saturation weighted harmonic average is appropriate (Biondi et al., 1998, Bentley, et al. 1999):

$$\frac{1}{K_f} = \frac{S_g}{K_g} + \frac{S_o}{K_o} + \frac{S_w}{K_w} \quad (3)$$

Where, S_g , S_o and S_w are the gas, oil and water saturations, respectively. In order to compute the bulk moduli of gas (K_g), oil (K_o) and water (K_w), the methods demonstrated by Batzle and Wang (1992) are applied. The fluid mixture density is a volume average given by:

$$\rho_f = S_g\rho_g + S_o\rho_o + S_w\rho_w \quad (4)$$

In order to estimate the dry bulk modulus, we have to use the two equations:

$$V_p = \sqrt{\frac{K_u + 4\mu/3}{\rho_u}} \quad (5)$$

$$V_s = \sqrt{\frac{\mu}{\rho_u}} \quad (6)$$

Here μ is the shear modulus of saturated rock. As V_p is known from the sonic log (Figure 5) and the V_p/V_s ratio of 1.9 derived from one dipole sonic logs in Pikes Peak area, we can obtain the values of K_u and μ based on equations. (5) and (6). Applying them to equation (1), the dry rock bulk modulus can be derived. In this case, we assume that the dry bulk modulus of rocks remains constant before and after production although slight differences of porosities exist between the drainage region and the undisturbed region. Finally, the Gassmann equation can be employed to calculate the saturated rock bulk modulus K_u and shear modulus under in-situ reservoir conditions after production. Table 1 shows the in-situ reservoir parameters before and after a 3-year production period provided by Sawatzky (ARC). Table 2 contains the physical properties of reservoir rock in the drainage regions before and after production calculated using the above formula. With a 10 percent gas saturation, the saturated rock bulk modulus dramatically drops from 10.6Gpa to 5.2Gpa , while the shear bulk modulus shows only a slight increase. Hence the P-wave velocity has decreased to 2325m/s from 2795m/s , and S-wave velocity has increased slightly due to the density decrease.

Table1 In-situ Reservoir Parameters of Cold Production in drainage regions

	Before Production	After Production
V_p (m/s) from logs	2795 m/s	unknown
V_p/V_s (from logs)	1.9	unknown
Density from log (g/cm^3)	2.16	unknown
Density of grain sand (g/cm^3)	2.65	2.65
Oil API	11.3	11.3
Specific gravity of pure methane	0.56	0.56
Gas pseudocritical temperature (F)	-116.5	-116.5
Gas pseudocritical pressure (Psi)	667	667
Solution Gas-Oil ratio	7.5	7.5
Reservoir temperature (C)	20	20
Reservoir pressure (kPa)	3000	1500
Water saturation (%)	20	20
Oil saturation (%)	80	70
Gas saturation (%)	0	10
Water salinity (ppm)	44000	44000
Porosity (%)	30	30

Table 2 Physical Properties of Drainage Region before and after Production

	before production	after production
	$S_g=0, S_o=0.8$	$S_g=0.1, S_o=0.7$
saturated rock bulk modulus (Gpa)	10.616	5.2252
saturated shear modulus (Gpa)	4.6726	4.6777
saturated bulk density (kg/m^3)	2156.5	2126.6
V_p (m/s)	2795	2325
V_s (m/s)	1472	1483

3. Time-Lapse Seismic Responses Of Cold Production Reservoir

Based on the two models before and after production shown in Figure 5 and 7, zero-offset seismic traces were generated using the exploding reflector in the Promax software package. The velocity and density grid is 1m by 1m. CDP intervals are 1 meter. Gaussian's wavelets have been applied to synthetic seismograms with dominant frequencies of 50Hz, 100 Hz and 200Hz, respectively. Figure 8 illustrates the seismic profiles with different frequencies of wavelets, as well as corresponding amplitude spectrums of the seismic traces at CDP 501.

In these Figures, we can observe the amplitude anomalies and traveltimes delays caused by the two drainage regions, where lower velocity and density exist compared with the ambient rocks. With the increase of the frequency bandwidths, we can see clearer and stronger amplitude anomalies and traveltimes delays. However, only when the frequency bandwidth reached 200Hz, the two drainage regions are clearly separated. Otherwise, the two thin drainage regions can only indicate the cumulative responses on the seismic sections. Considering these drainage regions as thin beds, the clear and detailed images of the amplitude anomalies corresponding to the drainage regions are determined by the seismic vertical resolution, which is related to the velocity of the drainage region and the frequency bandwidth. In our case, the highest vertical resolution is about 2.9m with a frequency bandwidth of 200Hz. That is the reason why we can distinguish these two drainage regions using 200Hz high frequency. For our model, the Fresnel zone is not an issue due to the diameter of the drainage regions being of order of 200 meters.

In order to understand the vertical resolution better, we modify the drainage model (Figure 7) to one net pay zone, keeping only the upper 5m drainage region, then changing the thickness to 3m and 1m, respectively. Figure 9 shows that the accumulative amplitude anomalies from 1m and 3m thick drainage regions can not be detected with a frequency bandwidth of 50Hz. Therefore, although it is important for the drainage regions to have a low velocity and a density to create amplitude anomalies, the seismic frequency bandwidth is necessarily needed to detect the amplitude anomalies.

Conclusions

The cold production process in heavy oil is a unique procedure of producing oil and sand simultaneously, while generating high permeability wormhole channels within the reservoir. The presence of wormholes with depleted pressures lead to significant changes in reservoir characters from the initial state of the reservoir. That makes seismic detection of drainage regions (production footprints) practical using time-lapse seismology techniques. The length of wormholes determines the extent of the drainage regions, also called depletion regions. Generally, the diameters of drainage regions cannot go too far away from the tip

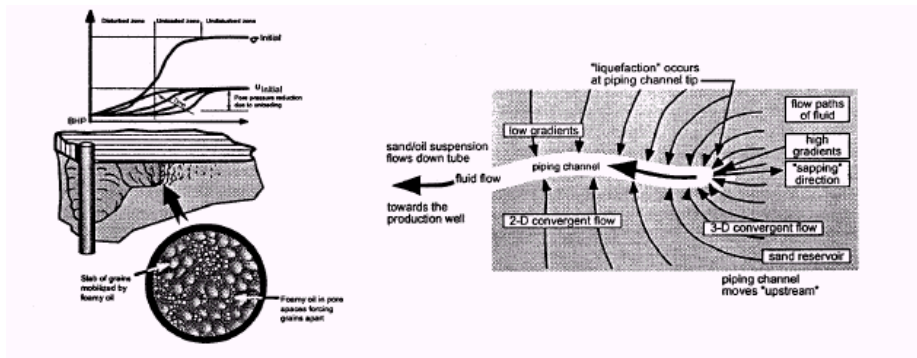
of wormholes. When reservoir pressures drop to the bubble point, the dissolved gas comes out of solution from the live oil, forming foamy oil. Hence, the exolved gas changed the fluid phases in the drainage regions, leading to P-wave velocity and density decreases. These physical properties cause “bright spots” on seismic responses. Since most net pays in cold production are less than 10m thick, seismic vertical resolution is a key detecting the images of drainage regions, which is determined by the velocity and the frequency bandwidth.

Acknowledgements

The authors thank the COURSE project and CREWES for their financial and technical support. We acknowledge the contributions to our research made by ARC. We also would like to thank Dr. Ron Sawatzky for his valuable suggestions and discussions.

References

- Batzle, M., and Wang, Z., 1992, Seismic properties of pore fluids, *Geophysics*, Vol 57, No. 11, P1396-1408.
- Bentley, L., and Zhang, J., 1999, Four-D seismic monitoring feasibility, CREWES Research Report, Vol.11.
- C-FER Report, 1994, Mechanisms and management of sand production, Vol. 2, 377.
- Domenico, 1976, Effect of brine-gas mixture on velocity in an unconsolidated sand reservoir, *Geophysics*, Vol.41, No.5, 882-894.
- Dusseault, M. 1994, Mechanisms and management of sand production, C-FER Project 88-06, Vol. 4.
- Gassmann, F., 1951, Elastic waves through a packing of spheres: *Geophysics*, 16, 637-685.
- Mayo, L., 1999, Seismic monitoring of foamy heavy oil, Lloydminster, Western Canada, 66th Ann. Internat. Mtg. Soc. Of Expl. Geophys, 2091-2094.
- Sawatzky, R.P. and Lillico, D.A., 2002, Tracking cold production footprints, CIPC, Conference, Calgary, Alberta, June 11-13.
- Tremblay, B., 1999, A review of cold production in heavy oil reservoirs, EAGE, 10th European Symposium on Improved Oil Recovery, Brighton, UK, August.



a) Foamy oil mechanism (C-FRE, 1994) b) Single propagating wormhole in a sandstone reservoir (Dusseault, 1994)
 Fig. 1: Foamy oil and wormhole networks in cold production reservoir

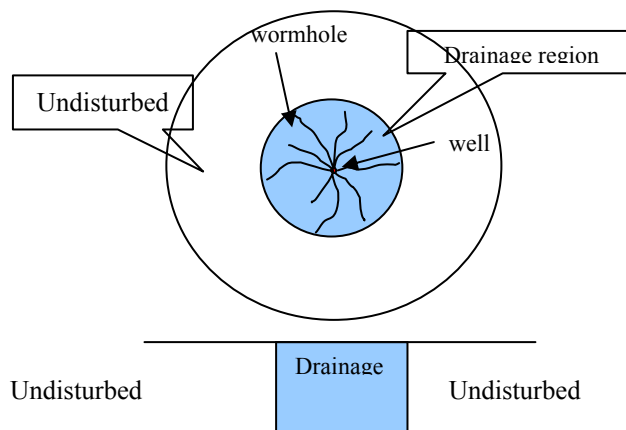


Fig. 2: 3D plane view (above) and 2D cross section of the drainage region

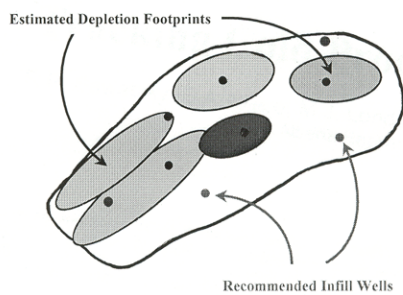


Fig. 3: Most likely depletion (drainage) footprint scenario for the cold production wells in the small southwest Saskatchewan heavy oil pool (Sawatzky, 2002)

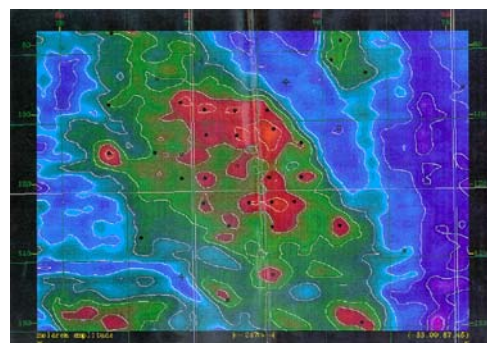


Fig. 4: Seismic amplitude extraction from the MacLaren horizon (Mayo, 1999). The 3D seismic program shot 9 years after the pool discovered. It shows amplitude anomalies.

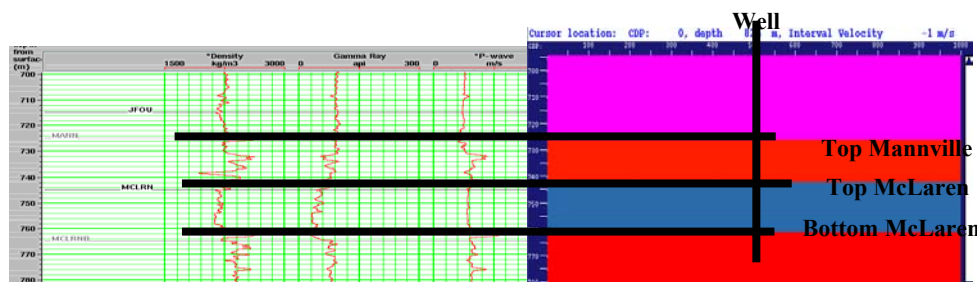


Fig. 5: Geological model of the initial reservoir before production from well log (Density, Gamma ray and V_p from left to right)

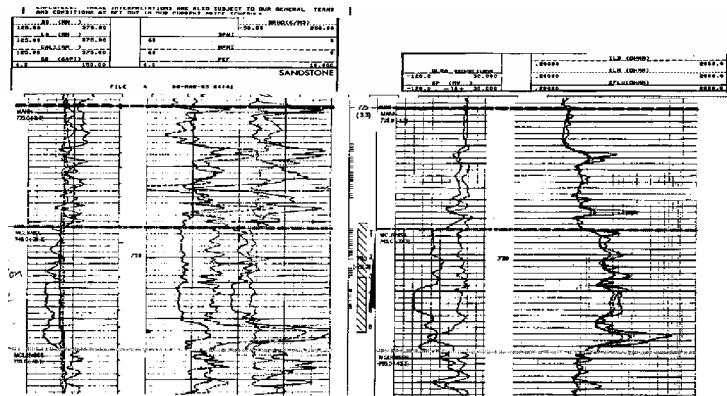


Fig. 6: Two main net pays (745-750m, 755-758m) in MacLaren reservoir sand, the upper one with 5m net pay, and the lower one with 3m

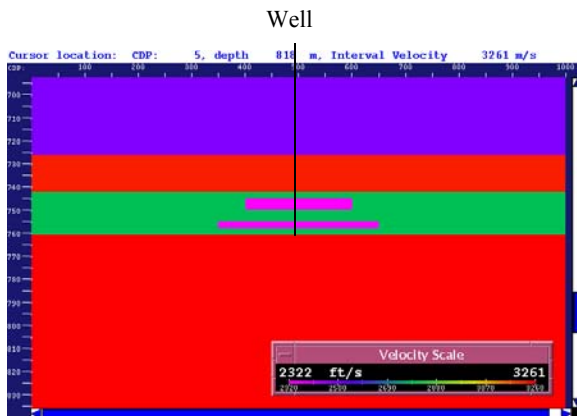
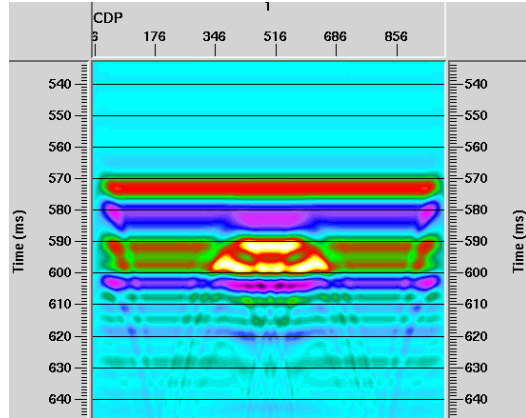
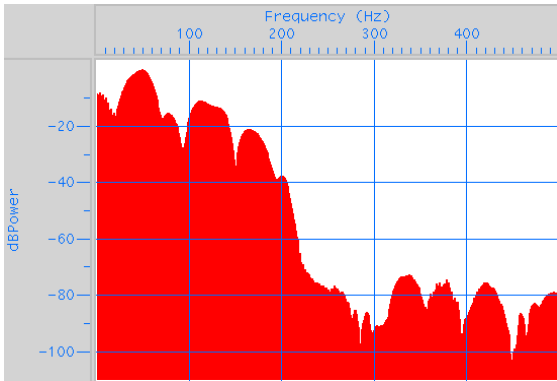
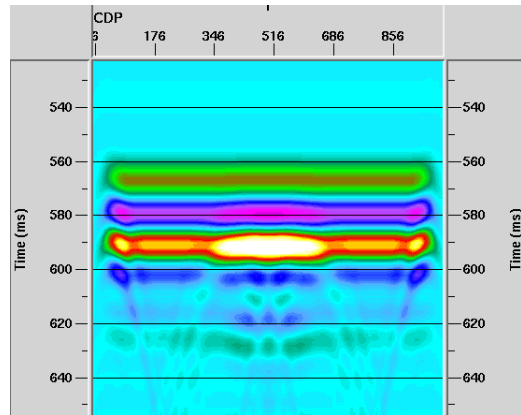
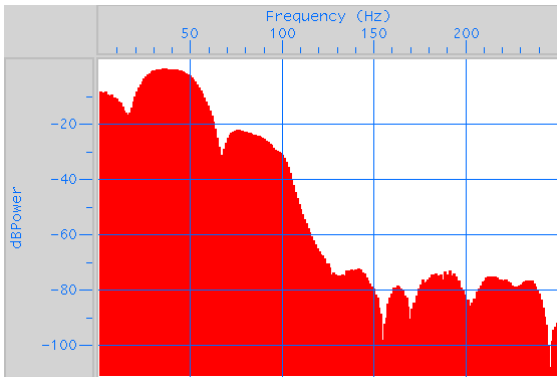


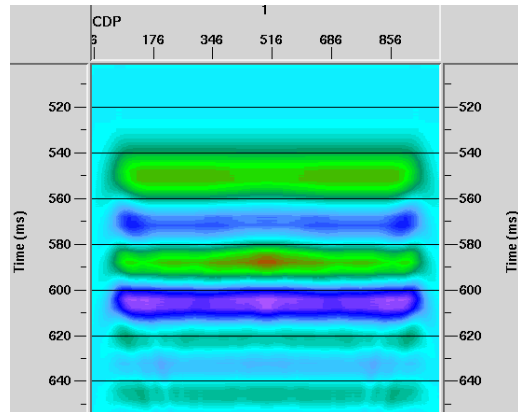
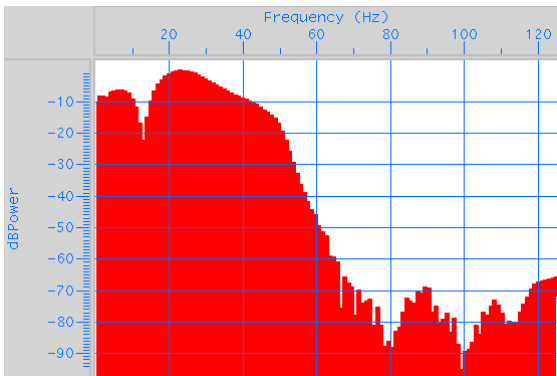
Fig. 7: The drainage region model after production within two net pays (upper one 5m thick with a diameter of 200m; the lower 3m thick, a diameter of 300m (in purple). Both have a velocity of 2325m/s, a density of 2.13g/cm³)



a) Amplitude spectrum (left) of trace at 501 CDP, and zero-offset seismic section (right) with a frequency bandwidth about 200Hz

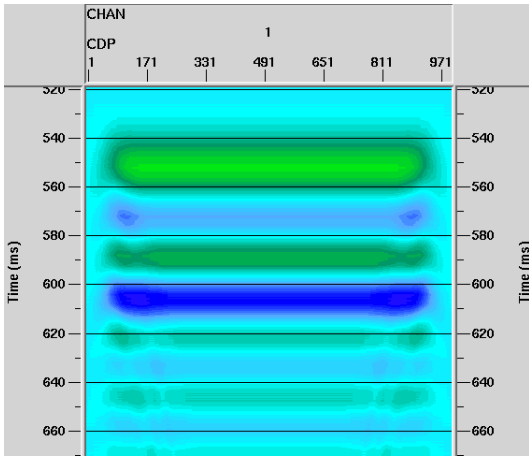


b) Amplitude spectrum (left) of trace at 501 CDP, and zero-offset seismic section (right) with a frequency bandwidth about 100Hz

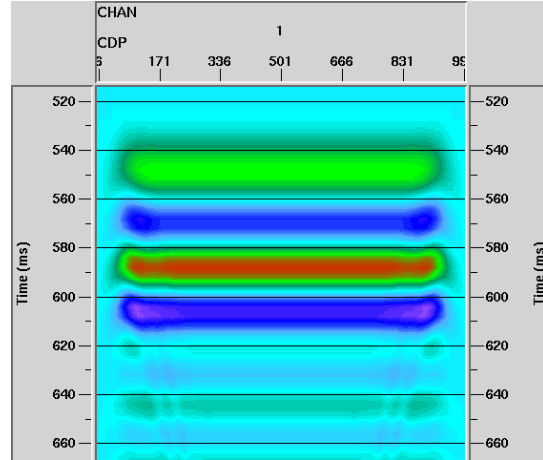


c) Amplitude spectrum (left) of trace at 501 CDP, and zero-offset seismic section (right) with a frequency bandwidth about 50Hz

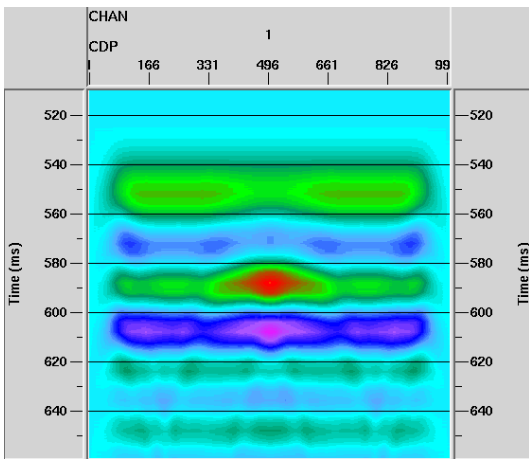
Fig. 8: Seismic responses of drainage regions with different seismic frequency bandwidths



(a)



(b)



(c)

Fig. 9: Seismic responses from modified model with one drainage region with a thickness (a) 1 meter, (b) 3 meters and (c) 5 meters using 50Hz frequency bandwidth